scientific reports

Check for updates

OPEN

Comparison of iPSC-derived human intestinal epithelial cells with Caco-2 cells and human in vivo data after exposure to *Lactiplantibacillus plantarum* WCFS1

Aafke W. F. Janssen[1,6], Benthe van der Lugt[1,6], Loes P. M. Duivenvoorde[1], Arjan Paul Vos[2], Shanna Bastiaan-Net[2], Monic M. M. Tomassen[2], Janine A. C. Verbokkem[2], Emmie Blok-Heimerikx[2], Guido J. E. J. Hooiveld[3], Peter van Baarlen[4], Laurent Ferrier[5] & Meike van der Zande[1]✉

To investigate intestinal health and its potential disruptors in vitro, representative models are required. Human induced pluripotent stem cell (hiPSC)-derived intestinal epithelial cells (IECs) more closely resemble the in vivo intestinal tissue than conventional in vitro models like human colonic adenocarcinoma Caco-2 cells. However, the potential of IECs to study immune-related responses upon external stimuli has not been investigated in detail yet. The aim of the current study was to evaluate immune-related effects of IECs by challenging them with a pro-inflammatory cytokine cocktail. Subsequently, the effects of *Lactiplantibacillus plantarum* WCFS1 were investigated in unchallenged and challenged IECs. All exposures were compared to Caco-2 cells and in vivo data where possible. Upon the inflammatory challenge, IECs and Caco-2 cells induced a pro-inflammatory response which was strongest in IECs. Heat-killed *L. plantarum* exerted the strongest effect on immune parameters in the IEC model, while *L. plantarum* in the stationary growth phase had most pronounced effects on immune-related gene expression in Caco-2 cells. Unfortunately, comparison to in vivo transcriptomics data showed limited similarities, which could be explained by essential differences in the study setups. Altogether, hiPSC-derived IECs show a high potential as a model to study immune-related responses in the intestinal epithelium in vitro.

The functions of the human intestinal tract go far beyond digestion and absorption of nutrients. The continuous exposure to foreign substances and the gut microbiota requires a unique and essential function of the intestine, i.e., keeping a fine balance between the internal and external environment. To this end, the intestine is equipped with a strong barrier, that has the complex task of tolerating the presence of resident microbiota on the one hand and protecting against potentially harmful substances and pathogens on the other hand[1]. The intestinal epithelium comprises a single layer of intestinal epithelial cells (IECs) that includes specialized cell types that act in concert to exert multiple tasks. For example, enterocytes are mainly responsible for the absorption of nutrients, Paneth cells exert host defense tasks and goblet cells are responsible for the production and secretion of mucus which forms a layer on top of the IECs that acts as a protective physical barrier and, amongst others, prevents direct contact between the intestinal microbiota and the IECs[2]. The connective tissue of the intestine contains a diverse set of innate and adaptive immune cells, which are responsible for the sensing, uptake, and transport of foreign antigens and for the subsequent presentation of antigens to adaptive immune cells that ultimately eliminate them[3]. Bacteria are particularly sensed via Toll-like receptors (TLRs) that are not only present on

[1]Wageningen Food Safety Research, Part of Wageningen University & Research, Akkermaalsbos 2, 6708 WB Wageningen, The Netherlands. [2]Wageningen Food & Biobased Research, Wageningen University & Research, Wageningen, The Netherlands. [3]Nutrition, Metabolism and Genomics Group, Division of Human Nutrition and Health, Wageningen University & Research, Wageningen, The Netherlands. [4]Host-Microbe Interactomics, Animal Sciences, Wageningen University & Research, Wageningen, The Netherlands. [5]Nestlé Institute of Health Sciences, Nestlé Research, Lausanne, Switzerland. [6]These authors share first authorship. ✉email: meike.vanderzande@wur.nl

immune cells, but are also constitutively expressed on IECs. Upon TLR activation in IECs, defensive responses are elicited, such as the secretion of cytokines, antimicrobial peptides (AMPs) and other immune factors[4]. A well-functioning intestinal barrier is crucial to maintain homeostasis, and impairment of the intestinal barrier function could have major consequences on human health, even beyond the gut[2].

To study human intestinal health and its potential disruptors in detail, representative and reproducible models are required. In vitro models provide useful alternatives for animal studies, which pose ethical considerations and difficulties in translation to the human in vivo situation. The human colorectal adenocarcinoma cell line Caco-2 is a well characterized and extensively used cell line. When grown and differentiated on permeable cell culture inserts into a homogeneous layer of enterocytes, Caco-2 cells offer a relatively simple model to study intestinal absorption, transport, and the integrity of the intestinal barrier[5,6]. However, the physiological relevance of this model to represent the highly complex intestinal architecture can be questioned, as it lacks the multicellular makeup present in the intestine in vivo. Furthermore, since Caco-2 cells are tumor-derived, they have accumulated mutations which may confound a phenotype of interest[7]. Caco-2 cells do not possess all functional TLRs[8], and have low basal expression of AMPs and cytokines, making them limited for studies investigating immune function[9–11]. A promising alternative for Caco-2 cells are human stem cell-derived intestinal models, like human induced pluripotent stem cell (hiPSC)-derived intestinal epithelial cells (IECs). hiPSC-derived IECs reflect the human intestinal tract more closely, as they comprise all the major intestinal cell types (i.e., enterocytes, stem cells, Goblet cells, Paneth cells and enteroendocrine cells)[12–15]. hiPSC-derived IECs possess the genomic variants of the donor, which might be healthy or containing specific mutations associated with a disease phenotype[16]. Like Caco-2 cells, hiPSC-derived IECs can be grown as monolayers on permeable inserts[15,17,18], making them convenient models for various metabolic and immune in vitro assays. Continued careful evaluation of model specific characteristics is key to better understand the potential and applicability domain of the model. We previously showed that hiPSC-derived IEC 2D monolayers are suitable to study transport of chemicals across the intestinal barrier[15]. Moreover, we showed that hiPSC-derived intestinal 3D organoids express CYP enzymes that are relevant for biotransformation studies, which are hardly or not expressed in Caco-2 cells[12]. However, the potential of hiPSC-derived IECs to study immune-modulatory responses has not been investigated yet. Therefore, the aim of the current study was to evaluate immune-related effects of hiPSC-derived IECs in comparison to Caco-2 cells. To this end, we first extensively characterized the immune response in both models after challenging them with a pro-inflammatory stimulus, i.e., a pro-inflammatory cytokine cocktail. In a second experiment, we investigated the effects of *Lactiplantibacillus plantarum* WCFS1 (previously known as *Lactobacillus plantarum*) in the hiPSC-derived IECs. For this experiment, both healthy and challenged cell models were exposed to *L. plantarum*. In the latter, cell models were first exposed to *L. plantarum* after which the pro-inflammatory cytokine cocktail was added. *L. plantarum* was selected as a case study as it has a safe history of use as a probiotic and it has been described to modulate immune responses with putative anti-inflammatory effects in humans[19]. In addition, gene expression data of the in vitro models were compared to gene expression data from a human in vivo study (i.e., from human duodenal samples collected after repeated ingestion of *L. plantarum* WCFS1*)*, which was described previously[20].

Materials and methods

Caco-2 cell culture

The human colorectal adenocarcinoma cell line Caco-2 (HTB-37), obtained from American Type Culture Collection (ATCC, Manassas, VA), was cultured in Dulbecco's Modified Eagle's Medium (DMEM, high glucose) supplemented with 10% heat-inactivated fetal bovine serum (Gibco, Thermo Fisher Scientific, Waltham, MA), 1% non-essential amino acids (Gibco) and 1% penicillin/streptomycin (Sigma) (further referred to as Caco-2 cell culture medium). Cells were kept in a humidified incubator at 37°C and 5% CO_2. Cells up to passage number 50 were used with a maximum difference of 10 passages and harvested at 80% confluence using Trypsin/EDTA (0.25%/0.05%; PAN Biotech, Aidenbach, Germany). To start differentiation, Caco-2 cells were seeded at a density of 4×10^5 cells/cm^2 in 12-well cell culture inserts with a polyester membrane (0.4 µm pore, Corning, New York, NY). The apical and basolateral compartments were filled with 500 µL and 1500 µL cell culture medium, respectively, and medium was refreshed every 2 to 3 days. Cells were differentiated for 21 days and monolayer integrity was determined by measuring transepithelial electrical resistance (TEER) using a Millicell-ERS Volt-Ohm meter (Millipore, Bedford, MA). Only monolayers with a minimum of 360 $\Omega \cdot$ cm^2 (after correction by subtracting the value of an empty Transwell insert) were used for experiments.

hiPSC culture and differentiation into IEC monolayers

The CS83iCTR-33n1 hiPSC cell line was obtained from the Cedars-Sinai Medical Center's David and Janet Polak Foundation Stem Cell Core Laboratory. This cell line was established through episomal reprogramming of fibroblasts of a 31-year-old healthy female. No karyotype abnormalities have been found for this cell line. hiPSCs were cultured on Matrigel-coated (Corning #354277) 6-well plates in mTeSR1 medium (STEMCELL Technologies, Vancouver, Canada) and were passaged using gentle cell dissociation reagent (STEMCELL Technologies). Cells up to passage number 45 were used with a maximum difference of 10 passages. An in-depth differentiation protocol was described previously[15]. Briefly, hiPSCs were dissociated into single cells, seeded in 24-well plates (220,000 cells/well) and differentiated towards definitive endoderm (DE). Subsequently, cells were differentiated to intestinal stem cells (ISCs), dissociated again and seeded on 12-well Transwell inserts with a polyester membrane (0.4 µm, Corning) coated with Growth Factor Reduced Matrigel (Corning #356231) at a density of 2.5×10^5 cells per insert. The cells were cultured for 12 days in differentiation medium (Advanced DMEM/F12 containing 2% fetal bovine serum, 1% non-essential amino acids (Gibco), 1×B27 (Gibco), 1×N2 (Gibco), 1% penicillin/streptomycin (Gibco) and 2 mM L-glutamine (Gibco)), supplemented with 20 ng/ml EGF, 30 µM forskolin, 5 µM 5-aza-2′-deoxycytidine (Sigma), 20 µM PD98059 (STEMCELL Technologies), and

0.5 µM A-83-01 (Sigma). This medium (further referred to as IEC culture medium) was used throughout the differentiation period and was refreshed every 2 to 3 days (400 µl apical and 1200 µl basolateral). Integrity of the hiPSC-derived IEC monolayer was determined by measuring transepithelial electrical resistance (TEER) using a Millicell-ERS Volt-Ohm meter (Millipore, Bedford, MA). Only IEC monolayers with a minimum of 150 $\Omega \cdot cm^2$ (after correction by subtracting the value of an empty Transwell insert) were used for experiments.

Lactiplantibacillus plantarum culture

Lactiplantibacillus plantarum WCFS1 (isolate of strain NCIMB8826) was cultured in MRS agar (Millipore) at 30 °C. Bacteria in the stationary phase (further referred to as stationary *L. plantarum*) were harvested and centrifuged at 5500 × g for 20 min, washed in PBS, centrifuged again at 6000 × g for 20 min and resuspended in 50 mL PBS to obtain a 10 × concentrated solution. Half of the bacteria were heat-killed by keeping them at 85 °C for 10 min. Stocks of stationary and heat-killed bacteria were made by resuspending 200 µL of the concentrated bacteria in 300 µL glycerol:demi-water (50% v/v; Sigma-Aldrich) and stored at -80 °C. At the day of the exposure, bacteria were thawed on ice, washed with PBS and centrifuged at 10,000 × g for 5 min. The pellet was then resuspended in either IEC or Caco-2 cell culture medium without antibiotics and diluted to 10^5 bacteria per mL. Bacterial concentration before and after exposure was measured using a method based on the most probable numbers (MPN) from serial dilutions. To this end, 90 µL of MRS was added to a 96-wells plate and inoculated with 10 µL of cell culture medium. Cells were serially diluted and incubated at 37 °C for 24 h. After 24 h the optical density was determined. Cut-off values for growth versus no growth were determined using negative controls. The MPN was determined based on the average value of 5 replicates. In addition, the survival of *L. plantarum* in IEC and Caco-2 cell culture medium was assessed by determination of colony forming units (CFUs). To this end, bacteria were added in a concentration of 10^5 bacteria per mL to a total volume of 5 mL antibiotics-free IEC or Caco-2 cell culture medium. After incubating for 48 h at 37 °C, 200 µL of medium was collected and serially diluted in Pepton physiologic salt solution (Tritium Microbiologie B.V.). 500 µL of the serial dilutions were plated in duplicate onto agar plates, anaerobically incubated overnight at 37 °C and colonies were counted.

Exposure to *L. plantarum*

Three days prior to exposure to *L. plantarum*, apical and basolateral medium of Caco-2 cells and IECs was replaced by antibiotics-free cell culture medium. On the first day of exposure, the heat-killed and stationary *L. plantarum* stocks were thawed on ice, washed with PBS and centrifuged at 10,000 × g. The pellet was resuspended in antibiotics-free cell culture medium, diluted to 10^5 bacteria/mL and added to the apical compartment of the Caco-2 and IEC cultures. Cells exposed to medium without bacteria served as control conditions. Cells were exposed to *L. plantarum* for 96 h. After 48 h, medium (and thus bacteria) was refreshed. The interval of medium renewal was kept equal for all experimental groups.

Inflammatory challenge

To evaluate the effects of an inflammatory challenge in both models, both hiPSC-derived IEC and Caco-2 cell models were exposed to a pro-inflammatory cytokine cocktail. This exposure was also given in parallel to the *L. plantarum* exposure where it was initiated after 24 h of exposure to *L. plantarum*. The inflammatory challenge comprised exposure to 2 ng/mL human Interferon-gamma (IFN-γ) protein (Bio-Techne) for 24 h, followed by exposure to 10 ng/ml human Tumor Necrosis Factor-alpha (TNF-α) protein and 1 ng/ml human Interleukin 1-beta (IL-1β) protein (both from Bio-Techne) for 48 h. Cells were exposed to these cytokines in both the apical and basolateral compartment. The cells exposed to this inflammatory challenge are further referred to as 'challenged'. Caco-2 cells and hiPSC-derived IECs kept on antibiotics-free cell culture medium without cytokines served as control conditions and are further referred to as 'healthy' models.

Lucifer Yellow translocation

Cell layer integrity after the pro-inflammatory challenge and/or *L. plantarum* exposure was measured using the fluorescent dye Lucifer Yellow (LY; Sigma-Aldrich). LY was dissolved in pre-heated cell culture medium at 0.5 mg/mL. Transwell inserts were placed in a new cell culture plate containing 1.2 (hiPSC-derived IECs) or 1.5 mL (Caco-2) cell culture medium in the basolateral compartment. The apical chamber was washed once with cell culture medium and subsequently filled with 0.4 (hiPSC-derived IECs) or 0.5 mL (Caco-2) medium containing LY. 50 µL aliquots were collected from the basolateral compartment and replaced with the same volume of IEC and Caco-2 cell culture medium at 30, 60, 90 120 and 150 min after addition of LY to the apical compartment. The concentration of LY in the test samples was calculated based on fluorometric readings (excitation wavelength 428 nm and emission wavelength 536 nm) using a standard curve of LY in cell culture medium. LY translocation was determined at a steady state flux of LY across the membrane (i.e., between 30 and 150 min after start of the exposure). After 150 min, all medium was collected from the apical and basolateral compartment. The apparent permeability coefficient (P_{app} in cm/s^{-1}) was calculated using the following equation:

$$P_{app} = \frac{dQ}{dt} \times \frac{1}{A \times C_0}$$

where A is the surface area (cm^2), dQ is the amount of the LY (nmol) transported over the steady state flux time interval dt (s) and C_0 is the initial LY concentration in the apical compartment (µM).

Quantification of IL-8, REG3α and HBD2 protein

Samples of apical and basolateral medium were collected from the Caco-2 cells and hiPSC-derived IECs at the end of the exposure experiment (i.e., after 72 h of exposure to the pro-inflammatory cytokine cocktail and after 96 h of exposure to *L. plantarum* with or without a pro-inflammatory stimulus). Medium samples were stored at -20 °C. Interleukin 8 (IL-8) (Thermo Fisher), Regenerating Family Member 3 Alpha (REG3α) (R&D systems) and Human Beta-defensin-2 (HBD2) (PeproTech, London, UK) ELISAs were all performed on all samples at the same day to prevent freeze–thaw cycles. ELISAs were performed according to the manufacturer's protocol.

DNA quantification

Cell density of the Caco-2 cells and IECs on Transwell inserts was determined at the end of the exposure experiment to normalize concentrations of IL-8, REG3a and HBD2 in the cell culture medium. Cells were lysed in 200 µL Trypsin/EDTA (TE)/DNA extraction buffer (containing 10 mM Tris, 1 mM EDTA and 0.2% (v/v) Triton X-100 (all from Sigma Aldrich); pH 8.0). The content of dsDNA in cell lysates in TE/DNA extraction buffer was measured using a Quant-iT PicoGreen dsDNA Assay Kit (Thermo Fisher Scientific). The assay was performed according to the manufacturer's protocol and dsDNA content was calculated as the amount of DNA (µg) per individual Transwell.

Cell viability

At the end of the exposure experiment, apical medium from the Caco-2 cells and hiPSC-derived IECs was collected on ice and used directly for extracellular lactate dehydrogenase (LDH) measurements as an indicator of cell death. For this, the Cytotoxicity assay (Promega, Leiden, the Netherlands) was used according to the manufacturer's protocol. Cell viability was determined using the WST-1 assay that determines the conversion of the tetrazolium salt WST-1 (4-[3-(4-iodophenyl)-2-(4-nitrophenyl)-2H-5-tetrazolio]-1,3-benzene disulfonate) to formazan by metabolically active cells. Cells were cultured specifically (although under similar conditions as the LDH assay) for the WST-1 assay. At the end of the exposure experiment, cells (on Transwell inserts) were exposed to WST-reagent (Sigma-Aldrich) at a 1:10 dilution in cell culture medium (200 µL apical and 600 µL basolateral) for 1 h. Per measurement, 3 wells without cells with only cell culture medium containing WST-1 reagent were taken along for background correction. After 1 h incubation at 37 °C and 5% CO_2, 75 µl (in duplicate) of each well (apical and basolateral separate) was transferred to a 96-well plate and absorbance at 450 nm was measured using a microplate reader (Synergy™ HT BioTek, Winooski, VT, USA). The background absorbance at 630 nm was subtracted. Cell viability was calculated based on the amount of formazan formation as a percentage of the formation in the healthy controls.

RNA isolation

RNA was extracted from Caco-2 cells and hiPSC-derived IECs using the RNeasy Mini Kit (Qiagen, Venlo, The Netherlands) at the end of the experiment. Total RNA was quantified using a Nanodrop (ND-1000, Thermo Scientific, Wilmington, Delaware, USA). For transcriptomics analysis, RNA integrity was analyzed using a total RNA Pico chip in an Agilent 2100 Bioanalyzer (Agilent Technologies).

cDNA synthesis and qRT-PCR

RNA (500 ng) extracted from the Caco-2 cells and hiPSC-derived IECs was used to synthesize cDNA using the iScript cDNA synthesis kit (Bio-Rad Laboratories, Veenendaal, The Netherlands). Subsequently, quantitative real-time reverse transcription-PCR (qRT-PCR) was performed using a CFX384 real-time PCR detection system (Bio-Rad Laboratories) using SensiMix (Bioline; GC Biotech, Alphen aan den Rijn, The Netherlands). The following cycles were performed: an initial denaturation of 95 °C for 10 min, followed by 40 cycles of denaturation at 95 °C for 10 s and annealing extension at 60 °C for 15 s. Finally, a melting curve was prepared (60 cycles of 10 s at 65 °C with an increase of 0.5 °C per 10 s). A standard curve using serial dilutions of pooled sample (cDNA from all samples), was taken along with every assay. Data were normalized against the geometrical mean of the reference genes *36B4* and *RPL27* and relative gene expression was calculated as a ratio relative to the expression of the healthy control group. Primer sequences were obtained from the Harvard PrimerBank[21] and ordered from Eurogentec (Liège, Belgium). Sequences of the used primers are listed in the Supplementary Methods.

RNA sequencing and data analysis

RNA sequencing was performed on 3 samples per experimental condition. RNA Library preparations and RNA sequencing were performed at Azenta Life Sciences (Leipzig, Germany). A detailed description of the RNA Library preparations and RNAseq, and the processing of RNAseq reads is given in the Supplementary Methods. RNAseq data is deposited in the NCBI Gene Expression Omnibus (GEO) (GSE276364).

To visualize multi-dimensional variation of the differentially expressed genes between the Caco-2 cells and hiPSC-derived IECs under healthy and challenged conditions exposed to either stationary or heat-killed *L. plantarum*, multidimensional scaling (MDS) plots were created using Limma (version 3.50.3). Differential gene expression in the two cell models was evaluated by comparison with the respective healthy control. Venn diagrams, showing the overlap of differentially expressed genes ($p < 0.05$ based on empirical Bayes moderated *t*-statistic) between IECs and Caco-2 cells under healthy and challenged conditions were made using the open access online tool Venny (version 2.1.0; https://bioinfogp.cnb.csic.es/tools/venny/). Additionally, heatmaps were made using Morpheus (https://software.broadinstitute.org/morpheus/) to visualize the differentially expressed genes (showing the respective genes' counts per million (cpm)) for the specific exposure conditions. In the heatmaps, gene expression was hierarchically clustered based on the Euclidean distance.

Ingenuity Pathway Analysis (IPA) was used to obtain insights in the potential biological mechanisms underlying the effects of an inflammatory challenge as well as *L. plantarum* exposure on hiPSC-derived IECs

and Caco-2 cells. To this end, canonical pathways and upstream regulators were analyzed. As input, lists were created containing gene identifiers (Ensembl Gene ID) together with the corresponding log2 fold changes and p-values. Cut-off criteria for p- values and log2 fold changes compared to healthy control were applied to meet the maximum input criteria of IPA. Only genes with a p-value below 0.05 were included. Furthermore, genes were selected with log2 fold changes below -0.5 and above 0.5, except for the gene lists of healthy versus challenged hiPSC-derived IECs and healthy versus challenged Caco-2 cells exposed to stationary *L. plantarum*, for which only genes were included with a log2 fold change below -1 and above 1.

Comparison in vitro and in vivo transcriptomics data

To compare the gene expression profiles of the IECs and Caco-2 cells with those obtained in vivo in humans, expression data from human duodenal biopsies exposed to various preparations of *L. plantarum* or control was obtained from the Gene Expression Omnibus (GSE11355). In short, this study entailed a randomized placebo-controlled cross-over study, in which eight healthy volunteers consumed a preparation with either stationary or heat-killed bacteria resuspended in maltodextrin solution or the placebo control (i.e., only the maltodextrin solution) every 30 min for a total duration of 6 h. Afterwards, biopsies of the duodenum were obtained from which total RNA was extracted. Microarray analysis was performed on a total of 24 samples (3 conditions for the eight individuals). An extensive description of experimental setup and details on the microarray analysis are given in the original research article[20]. Principal component analysis (PCA) was performed to get insights in (dis)similarities between the transcriptomics datasets from the current in vitro study (hiPSC-derived IECs and Caco-2 cells) and those from the in vivo study. To this end, datasets were integrated as described previously[22,23].

Statistical analysis

Data are expressed as mean ± SD. Statistical analyses (except for RNAseq analyses) were performed using GraphPad Prism (GraphPad Software, San Diego, USA). To determine statistically significant effects of the pro-inflammatory challenge, comparisons between challenged Caco-2 cells or hiPSC-derived IECs versus their respective healthy controls were analyzed by an unpaired Student's t-test. To determine statistically significant effects of the *L. plantarum* exposure in healthy and challenged Caco-2 or hiPSC-derived IEC models, a one-way ANOVA followed by Bonferroni post hoc analysis was used on data from the stationary or heat-killed *L. plantarum* exposure groups versus the respective healthy controls. To determine statistically significant effects of the *L. plantarum* exposure in challenged Caco-2 or hiPSC-derived IEC models versus *L. plantarum* exposure in healthy Caco-2 or hiPSC-derived IEC models a two-way ANOVA was used. A p-value below 0.05 was considered statistically significant.

Results

Evaluation of a hiPSC-derived IEC and Caco-2 model challenged by a pro-inflammatory stimulus

The first aim of this study was to characterize a hiPSC-derived IEC model that was challenged with a pro-inflammatory stimulus in order to induce an inflammatory-like state (so-called challenged conditions). Upon complete differentiation, hiPSC-derived IECs (further referred to as IECs) were exposed to a pro-inflammatory cytokine cocktail consisting of 2 ng/mL IFN-γ for 24 h, followed by exposure to 1 ng/mL IL-1β and 10 ng/mL TNF-α for another 48 h. In parallel, Caco-2 cells were exposed to the same stimuli for comparison. After exposure to the inflammatory challenge, TEER values were slightly lower in challenged IECs (not significant) and significantly lower in Caco-2 cells ($p < 0.001$) compared to the respective healthy controls (Fig. 1A). In line with these results, the apparent permeability coefficient (P_{app}) of LY was higher under challenged conditions in both cell models ($p < 0.05$ for IECs, not significant for Caco-2 cells; Fig. 1B), although the absolute P_{app} values were still low, i.e., in the range of low-permeable drugs[15]. Cell death, measured by LDH release, was slightly increased by the inflammatory challenge in both models (Figure S1A). However, cell density (in terms of DNA content) was unaffected or increased (Figure S1B), implying that the cell turnover rate might have been higher in both models.

Next, to verify if the pro-inflammatory challenge altered immune responses, transcriptomic analysis was performed on the IECs and Caco-2 cells. The challenge resulted in a number of 12,401 and 4,957 differentially expressed genes (DEGs) in the IEC and Caco-2 model, respectively. Ingenuity Pathway Analysis (IPA) identified the 'Pathogen Induced Cytokine Storm Signaling Pathway' as the most significantly enriched pathway in IECs and as the second most significantly enriched pathway in Caco-2 cells (Figure S1C). This pathway consists of 371 genes and is related to an uncontrollable inflammatory response induced by pathogens[24]. Out of the 371 genes in this pathway, a number of 85 and 72 genes were differentially expressed in the challenged IEC and Caco-2 model, respectively, compared to their healthy controls (Fig. 1C, Supplementary data 1). Furthermore, the top 10 most significantly enriched pathways mainly included pathways related to inflammation and immune modulation, indicating that challenging IECs and Caco-2 cells by a pro-inflammatory stimulus had the hypothesized effects of altering gene expression predominantly at the level of immune response. This result was confirmed by measuring the expression of a panel of genes related to intestinal inflammatory responses and antimicrobial activity using RT-qPCR, which showed that almost all genes were indeed significantly upregulated (Figure S1D–E). Also at protein level, the release of Interleukin 8 (IL-8), Regenerating Family Member 3 Alpha (REG3α) and Human Beta-defensin-2 (HBD2) was significantly higher in IECs under challenged conditions both apically and basolaterally (Fig. 1D, Figure S1F). In the challenged Caco-2 cells, secretion of IL-8 in the apical and basolateral compartment and secretion of HBD2 in the apical compartment were significantly higher, but the secretion of REG3α in the apical and basolateral compartment was unaffected (Fig. 1D and S1F).

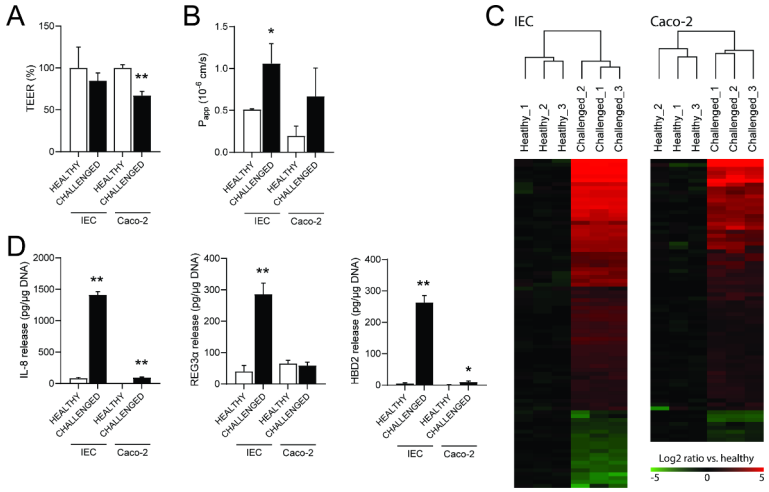

Fig. 1. Characterization of hiPSC-derived IEC and Caco-2 models challenged by an inflammatory stimulus compared to healthy, unchallenged cells. (**A**) Transepithelial electrical resistance (TEER) of IECs and Caco-2 cells, healthy or challenged with a pro-inflammatory cytokine cocktail for three days, expressed as percentage relative to its respective healthy control. (**B**) Apparent permeability coefficient (P_{app}) reflecting the flux of Lucifer Yellow from apical to basolateral direction. (**C**) Heatmap showing the hierarchically clustered significantly differentially regulated genes part of the 'Pathogen Induced Cytokine Storm Signaling Pathway' in healthy and challenged IECs and Caco-2 cells. (**D**) Release of Interleukin 8 (IL-8) in the basolateral compartment and the antimicrobial peptides Regenerating Family Member 3 Alpha (REG3α) and Human Beta-Defensin 2 (HBD2) in the apical compartment. Results are expressed as mean ± SD (N = 3). Statistically significant effects were analyzed by an unpaired Student's t-test. *$p < 0.05$; **$p < 0.001$ compared to the respective healthy controls.

Exposure of hiPSC-derived IECs and Caco-2 cells to *L. plantarum*

Next, the potential of IECs and Caco-2 cells to study host-microbe interactions was investigated by exposing the cell models to either stationary or heat-killed *L. plantarum* for 96 h (24 h prior and 72 h during the inflammatory challenge). An overview of the experimental design is displayed in Fig. 2A. Importantly, *L. plantarum* exposure was repeated after 2 days, because at that time point the cell culture medium containing IFN-γ had to be substituted with fresh medium containing IL-1β and TNF-α (Fig. 2A). For the exposure to stationary *L. plantarum*, bacterial counts on day 0 and 2 confirmed that the selected number of bacteria (i.e., 10^5 bacteria/mL) was added in both models on both timepoints (Fig. 2B). However, bacterial counts in the discarded medium at day 2 and 4 showed a massive decrease of bacteria in the IEC model, both under healthy and challenged conditions (Fig. 2B). In the Caco-2 model, the same trend was observed at day 2, although less pronounced, but no significant difference in *L. plantarum* was found at day 4 in the Caco-2 cell model under both healthy and challenged conditions (Fig. 2B). To investigate if the type of medium (IEC versus Caco-2 cell culture medium) was attributable to the observed differences in bacterial counts, the bacterial survival after growing *L. plantarum* in antibiotics-free IEC and Caco-2 cell culture medium was assessed. After 48 h, the bacterial survival was indeed lower in IEC medium compared to Caco-2 medium ($p < 0.05$) (Figure S2). This indicates that the lower number of *L. plantarum* in the IEC model compared to Caco-2 model could be (partly) explained by differences in cell culture medium.

Evaluation of *L. plantarum* exposure on cellular effects and barrier integrity in hiPSC-derived IECs and Caco-2 cells

In Caco-2 cells, exposure to stationary and heat-killed *L. plantarum* did not affect cell viability (measured using WST-1 and LDH assays; Figure S3A-B). Also in the IEC model, exposure to stationary and heat-killed *L. plantarum* did not affect cell viability using the WST-1 assay. LDH release even slightly decreased under challenged conditions ($p < 0.05$). The number of cells in all exposure groups remained unaffected with the exception of IECs exposed to heat-killed bacteria under challenged conditions, which showed a slight decrease in cell number (Figure S3C). Taken together, these data suggest that exposure to *L. plantarum* did not exert any cytotoxic effect on the intestinal cell models.

Next, the effects of *L. plantarum* exposure on intestinal barrier integrity were investigated. Exposure to heat-killed *L. plantarum* under both healthy and challenged conditions had no effect on intestinal permeability in both models (Figure S3D, E). Exposure to stationary *L. plantarum* also had no effect on intestinal permeability in the healthy and challenged IEC model, but surprisingly it caused a significant increase of TEER values in Caco-2 cells under both healthy and challenged conditions compared to the respective control conditions that were not exposed to *L. plantarum* (Figure S3D). However, these results were not reflected by P_{app} values, which were not significantly different but showed high variability (Figure S3E).

Exposure to heat-killed *L. plantarum* caused a significant increase in the release of IL-8 and REG3α in the IEC model under challenged conditions compared to the respective control ($p < 0.001$) (Fig. 3; Figure S4). In the Caco-2 model, the release of IL-8 in the basolateral compartment, but not the apical compartment, remained

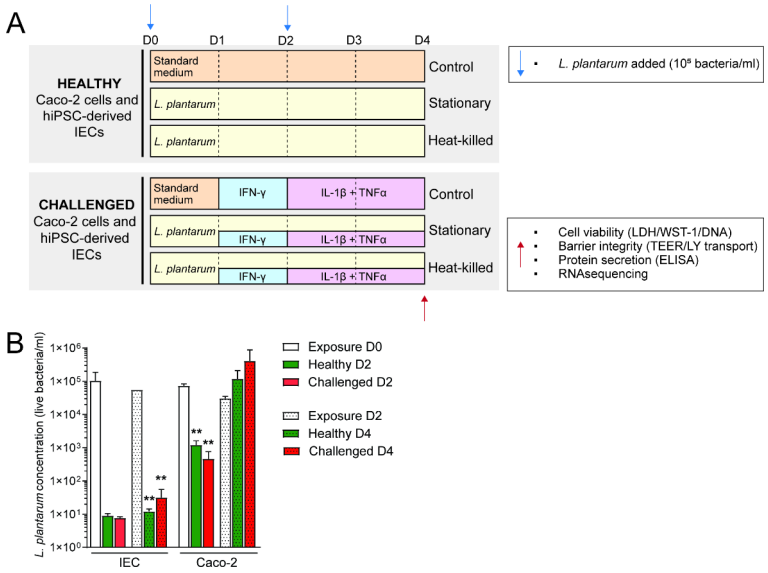

Fig. 2. Exposure of healthy and challenged hiPSC-derived IEC and Caco-2 models to *Lactiplantibacillus plantarum*. (**A**) Overview of experimental design displaying the time points at which hiPSC-derived IECs and Caco-2 were exposed to a pro-inflammatory cytokine cocktail and stationary or heat-killed *L. plantarum*. (**B**) Bacterial counts expressed as the concentration of live *L. plantarum* measured in cell culture medium of healthy and challenged IECs and Caco-2 cells. Live *L. plantarum* was quantified directly after exposure (D0), after two days (D2) and four days (D4). Results are expressed as mean ± SD (N = 3). Statistically significant effects were analyzed by a one-way ANOVA followed by a Bonferroni post hoc analysis. $^{**}p < 0.001$ compared to the respective controls, in this case the white bars.

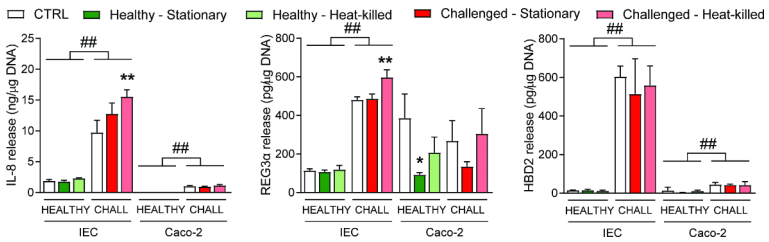

Fig. 3. Immune responses in healthy and challenged hiPSC-derived IEC and Caco-2 models after exposure to *Lactiplantibacillus plantarum*. Basolateral release of Interleukin 8 (IL-8) and apical release of the antimicrobial peptides Regenerating Family Member 3 Alpha (REG3α) and Human Beta-Defensin 2 (HBD2). Both cell models were exposed to either stationary or heat-killed *L. plantarum* and compared to the unexposed control condition (CTRL). Results are expressed as mean ± SD (N = 3). Statistically significant effects between healthy and challenged groups were analyzed by a two-way ANOVA and statistically significant effects within healthy and challenged groups were analyzed by a one-way ANOVA followed by a Bonferroni post hoc analysis. $^{*}p < 0.05$; $^{**}p < 0.001$ compared to the respective controls. $\#\#p < 0.001$ comparing healthy with challenged cell models.

unaffected (Fig. 3; Figure S4). REG3α release was significantly decreased in the apical compartment (Fig. 3), but not in the basolateral compartment (Figure S4) after exposure to stationary *L. plantarum* in Caco-2 cells under healthy conditions ($p < 0.05$). HBD2 release in both IECs and Caco-2 cells was unaffected after exposure to either stationary or heat-killed *L. plantarum* (Fig. 3; Figure S4).

Transcriptomics analysis of hiPSC-derived IECs and Caco-2 cells after *L. plantarum* exposure

To further explore the putative immune-related effects of *L. plantarum* on the IEC and Caco-2 cell models, transcriptomics analysis was performed. Additionally, the transcriptomics data of the in vitro models was compared with in vivo transcriptomics data obtained in a previous study by Van Baarlen and colleagues[20]. In short, in this randomized double-blind placebo-controlled cross-over study, 8 healthy volunteers consumed a maltodextrin solution containing different preparations of *L. plantarum* WCFS1 (including stationary and heat-killed) every 30 min for 6 h, after which duodenal mucosal biopsies were taken. Importantly, in the current study similar protocols were used to obtain the cultures of stationary and heat-killed *L. plantarum* that were used in the in vivo study.

Visualization by multidimensional scaling (MDS) showed a strong clustering of the samples (N = 3 per exposure group), which was mostly defined by the type of cell model (i.e., dim1 at 86%) and by the presence of the inflammatory challenge (dim2 at 5%; Fig. 4A). A closer look into the two cell models separately did not reveal clustering defined by *L. plantarum* exposure in IECs. In contrast, in the Caco-2 cell model a clear separation of samples exposed to stationary *L. plantarum* was observed under both healthy and challenged conditions (Fig. 4B). Exposure to stationary *L. plantarum* significantly altered the expression of 1,517 and 1,575 genes in healthy and challenged IECs, respectively ($p < 0.05$). A considerably higher number of genes was significantly differentially expressed upon exposure to stationary *L. plantarum* in the Caco-2 cells, i.e., 11,266 under healthy conditions and 10,864 under challenged conditions (Fig. 4C). Approximately 7% of the DEGs overlapped between the IEC and Caco-2 model, regardless of the exposure to the inflammatory challenge (Fig. 4D). To investigate the biological implications of the DEGs after exposure to stationary *L. plantarum*, upstream regulator analysis was performed using IPA. Upstream regulator analysis identifies potential regulators that might be responsible for downstream changes in gene expression and gives a prediction of their activation status by a positive or negative z-score, where a z-score between -2 and 2 is considered not biologically relevant. The top 20 potential upstream regulators (based on the lowest p-value) for each healthy and challenged cell model is displayed in Fig. 5. In the IEC model under healthy conditions, 4 activated and 7 inhibited upstream regulators were found, and 3 activated and 3 inhibited upstream regulators were found under challenged conditions (Fig. 5). The number of activated upstream regulators was higher in Caco-2 cells as 16 and 9 upstream regulators were activated under healthy and challenged conditions, respectively (Fig. 5). Most of the activated upstream regulators were related to regulation of immune responses. Additionally, canonical pathway analysis was performed in IPA which identified 'Pathogen induced cytokine storm signaling pathway' and 'Leukocyte migration' as the most affected immune-related pathways in Caco-2 cells. To visually assess the impact of stationary *L. plantarum* on these pathways in Caco-2 cells versus the IEC model, the genes within these pathways were identified and hierarchically clustered in a heatmap (Fig. 6A-B, Supplementary data 2). A clear differential expression of genes present in these pathways was observed in Caco-2 cells exposed to stationary *L. plantarum,* irrespective of whether the Caco-2 cells were subjected to a challenge or not (Fig. 6A, B). These results imply that in Caco-2 cells, the high number of differentially expressed genes in the groups exposed to stationary *L. plantarum* (Fig. 4B) might be predominantly explained by an altered immune response. Exposure of Caco-2 cells to heat-killed *L. plantarum* had a considerably milder effect on Caco-2 gene expression than the stationary variant, demonstrated by the

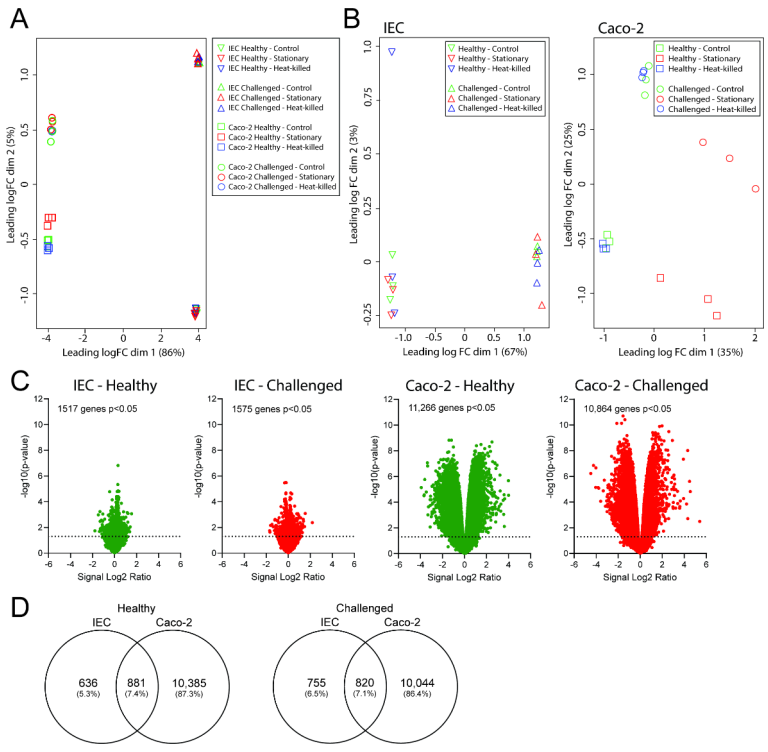

Fig. 4. Transcriptomic analysis of healthy and challenged hiPSC-derived IEC and Caco-2 models after exposure to stationary or heat-killed *Lactiplantibacillus plantarum*. (**A**) Multidimensional scaling (MDS) plot including all exposed groups. (**B**) MDS plot of the IEC and Caco-2 models separately. (**C**) Volcano plots showing differentially expressed genes in healthy and challenged IEC and Caco-2 models exposed to stationary *L. plantarum*, compared to the control (expressed as Signal log2 ratio) plotted against statistical significance (expressed as -log10 *p* value of empirical Bayes moderated *t*-statistic *p* value). The dashed line represents the significance level of $p = 0.05$ (**D**) Venn diagrams representing the overlap in significantly differentially expressed genes ($p < 0.05$) between IECs and Caco-2 cells under healthy and challenged conditions.

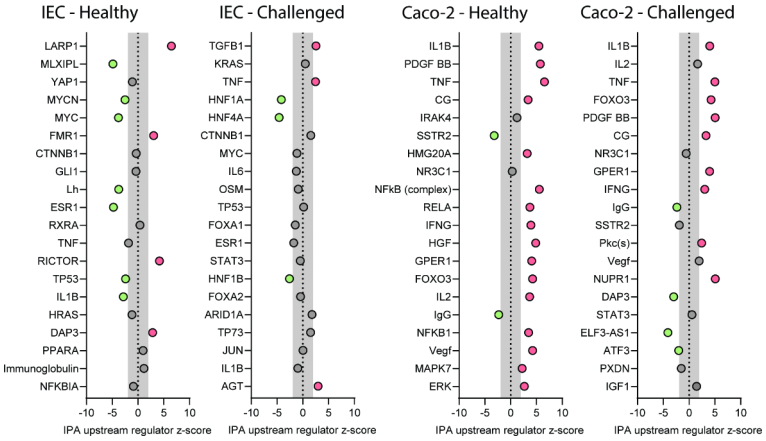

Fig. 5. Upstream Regulator analysis by Ingenuity Pathway Analysis (IPA) of hiPSC-derived IEC and Caco-2 models exposed to stationary *Lactiplantibacillus plantarum*. The top 20 upstream regulators are listed in the order of significance level (p-value of overlap). The IPA upstream regulator z-score indicates the predicted activation level, with either positive (red dot) or negative (green dot) values indicating an activated or inhibited regulator, respectively. Z-scores between -2 and 2 are considered not biologically relevant (grey zone).

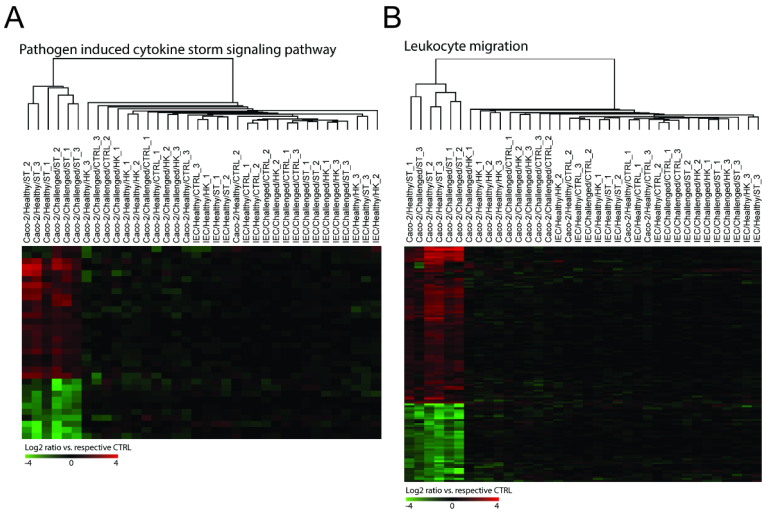

Fig. 6. Hierarchical clustering of genes part of immune-related pathways. Heatmap displaying genes part of the immune-related pathways 'Pathogen induced cytokine storm signaling pathway' (32 genes) and 'Leukocyte migration' (120 genes) in IEC and Caco-2 models exposed to heat-killed or stationary *L. plantarum*. Expression is normalized against average expression of its respective unexposed control.

lower (~20-30x) number of DEGs on the one hand (i.e., 506 genes under healthy conditions and 312 genes under challenged conditions) (Figure S5A, B) and negligible activation of upstream regulators on the other hand (Figure S6). In IECs, exposure to heat-killed *L. plantarum* resulted in 1,868 and 1,515 differentially regulated genes under healthy and challenged conditions, respectively (Figure S5). The numbers and types of activated and inhibited upstream regulators were comparable to those in the stationary *L. plantarum* exposure group (Fig. 5 and Figure S6). While the numbers of DEGs and upstream regulators were comparable, it should be noted that there was little overlap in DEGs in the IECs between the exposure to heat-killed and stationary *L. plantarum*. The percentage of overlapping genes between Caco-2 cells and IECs was approximately 2% under both healthy and challenged conditions. Altogether, these results show that the IEC and Caco-2 cell models differ substantially at the transcriptomics level, with the most pronounced effects related to immune response in Caco-2 cells exposed to stationary *L. plantarum*.

Next, transcriptomics data from the in vitro models was compared with transcriptomics data obtained in the in vivo study performed by Van Baarlen et al.[20]. Principal component analysis (PCA) showed that the samples from the in vivo study, IEC model and Caco-2 model were clearly separated (PC2 at 15.2%) (Fig. 7). Strikingly, in the in vivo samples, no clear effects of stationary and heat-killed *L. plantarum* was observed (Fig. 7), which might be due to interindividual variation between the donors. A clear clustering of the samples based on technique was observed, i.e., microarray (in vivo study) and RNAseq (in vitro models) (PC1 at 77.01%) (Figure S7). With

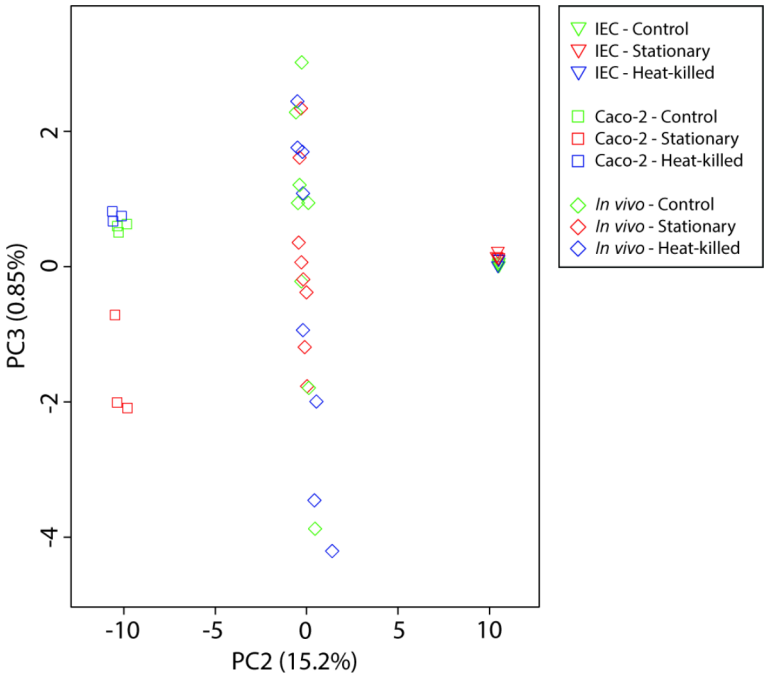

Fig. 7. Comparison of in vitro and in vivo transcriptomics data using principal component analysis (PCA). PCA plot showing PC2 and PC3, including the samples of the healthy in vitro models (i.e., IEC and Caco-2 cell models) and samples from the in vivo study performed by Van Baarlen et al.[20].

regard to the number of DEGs, a striking difference was found after exposure to stationary and heat-killed *L. plantarum*, when comparing the in vivo and in vitro studies. In the in vivo study, about 400 and 700 genes were differentially expressed ($p < 0.05$) after consumption of stationary and heat-killed *L. plantarum*, respectively[20], while these numbers were substantially higher in the in vitro studies (Fig. 4C, D and S5A, B).

Effects of *L. plantarum* on the expression of NF-kB subunits and antagonists in healthy and challenged IECs and Caco-2 cells

One of the major findings in the in vivo study by Van Baarlen and colleagues was that heat-killed and stationary *L. plantarum* caused differential regulation of NF-κB subunits and antagonists with the largest effects for heat-killed bacteria. For this reason, the expression profiles of genes encoding NF-κB subunits and antagonists of the in vivo study were compared with the gene expression profiles obtained in the in vitro studies presented here. In IECs under both healthy and challenged conditions, the expression of most of this gene panel was not significantly differentially regulated, and the genes that were significantly differentially expressed had low effect sizes (Supplementary Table 1). On the contrary, the complete panel of genes was significantly differentially regulated in Caco-2 cells exposed to stationary *L. plantarum* under both healthy and challenged conditions (Supplementary Table 2). Apart from *NFKB1 (p50)*, which was downregulated (fold change = -1.51), all other genes were upregulated (fold change between 1.50 and 3.46). Strikingly, exposure to heat-killed *L. plantarum* did not induce any significant changes in gene expression of this particular gene panel in Caco-2 cells, while the heat-killed bacterium exhibited most prominent effects in the in vivo study.

Discussion

The aim of the current study was to evaluate the potential of a hiPSC-derived IEC model to study immune-related effects and to compare it with the commonly used human colonic adenocarcinoma cell line Caco-2, and with data obtained from a human in vivo study. First, we focused on characterization of the in vitro models after exposure to an inflammatory challenge to investigate their capacity to elicit immune responses that resemble to inflammatory-like response. Second, the challenged model was used to investigate the potential anti-inflammatory properties of the probiotic *L. plantarum*. The pro-inflammatory challenge that was used consisted of a 24-h pre-stimulus with IFN-γ followed by 48 h exposure to IL-1β and TNF-α. These exposure conditions were based on previous reports[25–27] and were optimized in hiPSC-derived IECs and Caco-2 cells in several pilot experiments (data not shown). IFN-γ served as pre-stimulus to prime the cells to respond to TNF-α by upregulating TNF-α receptors, which in turn mediates barrier dysfunction[26,27]. IL-1β and TNF-α induced the inflammatory response. Both cell models showed comparable trends in intestinal permeability and immune responses after the pro-inflammatory challenge. Previous studies applying the same cytokines also showed increased intestinal permeability in vitro as well as in vivo[26–28]. We found that the intestinal permeability was slightly increased in both models, but was not affected to such an extent that it indicated major disruption of the intestinal barrier. A highly compromised intestinal barrier after exposure to pro-inflammatory cytokines would not reflect a physiologically relevant situation and would hamper an accurate interpretation of the results.

Transcriptomics analysis and inflammatory marker read-outs showed that both models were capable of inducing an inflammatory-like response, thereby demonstrating that the models appear suitable for studying immune-modulatory effects. The IEC model seemed to be more responsive to the inflammatory challenge than the Caco-2 model given the stronger induction of IL-8 and AMPs, both at gene- and protein expression level. These differences might be explained by the fact that, in contrast to Caco-2 cells, IECs contain multiple cell types, including Paneth cells which are mainly responsible for the production of AMPs. The inflammatory-like state that was created can be considered an important addition to study the effects of potential anti-inflammatory properties of compounds or substances, including probiotics.

When exposed to live *L. plantarum,* strikingly, in the IEC model a major decrease in the number of live bacteria was found compared to the Caco-2 model after 2 and 4 days of exposure. This decrease was observed in IECs both under healthy and challenged conditions, indicating that this observation cannot be explained by the increased release of the AMPs REG3α and HBD2 after exposure to the inflammatory challenge (Fig. 3). However, we did find higher basal expression values of genes encoding a panel of other AMPs (i.e., Human Beta-Defensin 1 (HBD1), phospholipase A2 group IIA (sPLA2), C–C Motif Chemokine Ligand 20 (CCL20), Lysozyme (LYZ)) in unexposed IECs compared to Caco-2 cells (Supplementary Table 3), which might explain the reduced live bacterial counts in IECs. Another factor that could explain the decreased counts of *L. plantarum* is the different composition of the cell culture media used for the Caco-2 and IEC models (i.e., DMEM and Advanced DMEM/F12, respectively). These media have approximately 4× to 6× lower glucose contents, for DMEM and Advanced DMEM/F12 respectively, than MRS medium in which *L. plantarum* was cultured. Since lactobacilli use glucose as energy source[29], a lower availability of glucose in IEC medium may lead to a decrease in live bacterial counts. Indeed, we observed a lower bacterial survival in IEC medium (only medium, so without cells) after culturing the bacteria for 48 h in comparison to culturing them in Caco-2 medium ($p < 0.05$) (Figure S2). This suggests that the relatively low glucose content might have played a role in the observed decrease in *L plantarum* survival during exposure to IECs. Another factor that might explain the difference in bacterial counts between the IEC and Caco-2 model is the presence of a mucus layer in IECs. Previously we extensively characterized this hiPSC-derived IEC model using gene expression analysis and immunofluorescence staining to show the presence of mucus and goblet cells[15]. An important function of the mucus layer is protecting the intestinal epithelial cell layer to bacterial infiltration by immobilizing bacteria[30] and it is a framework to which certain bacteria, including *Lactobacillus* species, can adhere to[31]. Thus, a fraction of *L. plantarum* might have been immobilized in the mucus layer of the IECs and was therefore not included in the measurement of bacterial counts. Nevertheless, we did find marked effects in both IECs and Caco-2 cells after exposure to *L. plantarum* compared to control samples, indicating that, although we measured lower bacterial counts than originally anticipated (mainly in the IECs), *L. plantarum* did induce biological effects.

Exposure to stationary or heat-killed *L. plantarum* did not appear to have marked effects on barrier integrity and cell viability. These results are in line with previous studies showing that *L. plantarum* is not cytotoxic for Caco-2 cells[32] and other cell lines[33]. Moreover, *L. plantarum* as a probiotic bacterium is recognized as safe to use in humans[34]. To evaluate the effects of *L. plantarum* exposure in the IEC and Caco-2 models on a more detailed level, transcriptomics analysis was performed. Gene expression profiles in both models differed substantially, and most pronounced effects were observed in Caco-2 cells exposed to stationary *L. plantarum*. This was reflected by a high number of DEGs and predominantly increased activation of upstream regulators related to immune responses. Heat-killed *L. plantarum* exerted a substantial weaker effect on Caco-2 cells than stationary *L. plantarum* upon exposure, with a considerably lower number of DEGs (i.e., 506 and 312 genes for heat-killed bacteria versus 11,266 and 10,864 genes for the stationary variant under healthy and challenged conditions, respectively). Compared to Caco-2 cells, a higher number of DEGs was found in IECs after exposure to heat-killed *L. plantarum* (i.e., 1,868 and 1,515 genes in IECs under healthy and challenged conditions, respectively), indicating that IECs might potentially be more responsive to exposure to heat-killed *L. plantarum* than Caco-2 cells. After exposure of IECs to stationary *L. plantarum*, 1,517 and 1,575 DEGs were found under healthy and challenged conditions, respectively. However, no big differences in effects on upstream regulators connected to immune responses were found. Interestingly, exposure to heat-killed *L. plantarum* under challenged conditions significantly increased IL-8 and REG3α release in IECs, while this effect was absent after exposure to *L. plantarum* in the stationary phase. Comparable results were found in vivo, where heat-killed *L. plantarum* induced gene expression profiles related to immune responses to a higher extent than its stationary counterpart. It was hypothesized that the more pronounced inflammatory effects were triggered by exposure to components of the cell wall released after heat-treatment of *L. plantarum,* rather than the intact cell wall of live *L. plantarum*[20]. An important difference between the in vitro models that should be taken into account is the fact that Caco-2 cells not only consist of one cell type, but also lack a mucus layer, resulting in more physical contact of *L. plantarum* to the cells. This might explain the more prominent effect of stationary *L. plantarum* on gene expression compared to IECs. Moreover, immune-modulatory effects of probiotics are often mediated via TLRs which, upon activation, initiate the release of signaling molecules that trigger the underlying immune tissue[1,35]. It was previously shown that Caco-2 cells do not have all (functional) TLRs present[8]. While out of the scope for this paper, future research should focus on the presence and functionality of TLRs in hiPSC-derived IECs to be able to draw further conclusions on TLR-mediated immune responses in IECs.

In vivo, *L. plantarum* has been described to have immune-modulatory properties including induction of immune tolerance[36]. Gene expression profiles in the in vivo study by Van Baarlen and colleagues showed upregulation of NF-κB subunits and NF-κB antagonists by both stationary and, to a higher extent, heat-killed *L. plantarum*[20]. In the present study, the expression of the same set of genes was not differentially regulated in the IECs (Supplementary Table 1), implying that the regulation of NF-κB-dependent pathways was different between the in vitro IEC model compared to the in vivo situation. Daghero et al.[37] have recently established NF-κB reporter organoids from different segments of the murine intestine. Interestingly, exposure of these

organoids to *L. plantarum* ATCC8014 did not trigger any activation of NF-κB pathway per se, while it was able to decrease TNF-α-induced signaling. In addition, duodenal biopsies used in the study by Van Baarlen et al.[20] are likely to include immune cells besides epithelial cells. Murine immune cells (RAW264 macrophage cell line) have been shown to react to *L. plantarum* JCM8341 extracellular vesicles, with a strong activation of NF-κB pathway[38]. Remarkably, in Caco-2 cells exposed to stationary *L. plantarum* WCFS1, the expression of NF-κB subunits and antagonists was to a certain extent comparable with the in vivo study. However, while stationary *L. plantarum* had the most pronounced effects on Caco-2 cells, in the in vivo study most pronounced effects were found after exposure to heat-killed *L. plantarum*. Moreover, the significant downregulation of *NFKB1 (p50)* in Caco-2 cells emphasizes another important discrepancy with the in vivo study. Clearly, both in vitro models showed differences when compared to the in vivo data. This is likely due to essential differences in study setups of the in vitro and in vivo studies which hamper a one-to-one comparison of the data. First, in the current study RNA sequencing was performed, while gene expression analysis in the in vivo study was performed using microarrays. Next, both the dose as well as the exposure time of *L. plantarum* differed between the in vitro and in vivo studies. Moreover, the duodenal samples used in the in vivo study provided a complete representation of all cell types present in the human intestine, including immune cells. The absence of immune cells in both in vitro models hampers a complete biological interpretation of host-microbe interactions. In order to overcome this, it might be worthwhile to investigate the potential of an IEC model in co-culture with immune cells, such as dendritic cells derived from human peripheral blood mononuclear cells (PBMCs). To the best of our knowledge, no such co-cultures using hiPSC-derived IECs have been described in literature yet, although co-cultures of intestinal epithelial cells, including Caco-2 cells, with immune cells have been established previously[39]. The IEC model reflects the cellular and physiological complexity of the intestine in vivo more accurately than the Caco-2 cell model, and shows high responsiveness to pro-inflammatory stimuli. Therefore, this is a very promising model to study immune responses upon a wide variety of external stimuli. Still, important steps can be made by further characterizing the IEC model in terms of expression and functionality of TLRs and by adding an immune component to the model to better recapitulate immune responses in the intestine. Furthermore, future studies could also include hiPSCs derived from different donors, which allows to study populational variation in vitro.

Data availability

Gene expression data of the current study is available in the NCBI Gene Expression Omnibus (GEO) (GSE276364). Gene expression data of the in vivo study by Van Baarlen et al. is available in the GEO (GSE11355). Other data that support the findings of this study are available from the corresponding author upon request.

Received: 15 July 2024; Accepted: 30 September 2024
Published online: 02 November 2024

References

1. Allaire, J. M. et al. The intestinal epithelium: Central coordinator of mucosal immunity. *Trends Immunol.* **39**, 677–696. https://doi.org/10.1016/j.it.2018.04.002 (2018).
2. Turner, J. R. Intestinal mucosal barrier function in health and disease. *Nat. Rev. Immunol.* **9**, 799–809. https://doi.org/10.1038/nri2653 (2009).
3. Mowat, A. M. & Agace, W. W. Regional specialization within the intestinal immune system. *Nat. Rev. Immunol.* **14**, 667–685. https://doi.org/10.1038/nri3738 (2014).
4. Pardo-Camacho, C., González-Castro, A. M., Rodiño-Janeiro, B. K., Pigrau, M. & Vicario, M. Epithelial immunity: priming defensive responses in the intestinal mucosa. *Am. J. Physiol. Gastrointest. Liver Physiol.* **314**, G247-g255. https://doi.org/10.1152/ajpgi.00215.2016 (2018).
5. Lopez-Escalera, S. & Wellejus, A. Evaluation of Caco-2 and human intestinal epithelial cells as in vitro models of colonic and small intestinal integrity. *Biochem. Biophys. Rep.* **31**, 101314. https://doi.org/10.1016/j.bbrep.2022.101314 (2022).
6. Ding, X. et al. Differentiated Caco-2 cell models in food-intestine interaction study: Current applications and future trends. *Trends Food Sci. Technol.* **107**, 455–465. https://doi.org/10.1016/j.tifs.2020.11.015 (2021).
7. Ilyas, M., Tomlinson, I. P., Rowan, A., Pignatelli, M. & Bodmer, W. F. Beta-catenin mutations in cell lines established from human colorectal cancers. *Proc. Natl. Acad. Sci. USA* **94**, 10330–10334. https://doi.org/10.1073/pnas.94.19.10330 (1997).
8. Grouls, M., van der Zande, M., de Haan, L. & Bouwmeester, H. Responses of increasingly complex intestinal epithelium in vitro models to bacterial toll-like receptor agonists. *Toxicol. In Vitro* **79**, 105280. https://doi.org/10.1016/j.tiv.2021.105280 (2022).
9. Fusco, A., Savio, V., Donniacuo, M., Perfetto, B. & Donnarumma, G. Antimicrobial peptides human beta-defensin-2 and -3 protect the gut during *Candidaalbicans* infections enhancing the intestinal barrier integrity: In vitro study. *Front Cell Infect. Microbiol.* **11**, 666900. https://doi.org/10.3389/fcimb.2021.666900 (2021).
10. Hosoi, T. et al. Cytokine responses of human intestinal epithelial-like Caco-2 cells to the nonpathogenic bacterium Bacillus subtilis (natto). *Int. J. Food Microbiol.* **82**, 255–264. https://doi.org/10.1016/s0168-1605(02)00311-2 (2003).
11. Parlesak, A., Haller, D., Brinz, S., Baeuerlein, A. & Bode, C. Modulation of cytokine release by differentiated CACO-2 cells in a compartmentalized coculture model with mononuclear leucocytes and nonpathogenic bacteria. *Scand. J. Immunol.* **60**, 477–485. https://doi.org/10.1111/j.0300-9475.2004.01495.x (2004).
12. Janssen, A. W. F. et al. Cytochrome P450 expression, induction and activity in human induced pluripotent stem cell-derived intestinal organoids and comparison with primary human intestinal epithelial cells and Caco-2 cells. *Arch. Toxicol.* **95**, 907–922. https://doi.org/10.1007/s00204-020-02953-6 (2021).
13. Spence, J. R. et al. Directed differentiation of human pluripotent stem cells into intestinal tissue in vitro. *Nature* **470**, 105–109. https://doi.org/10.1038/nature09691 (2011).
14. Tamminen, K. et al. Intestinal commitment and maturation of human pluripotent stem cells is independent of exogenous FGF4 and R-spondin1. *PLoS ONE* **10**, e0134551. https://doi.org/10.1371/journal.pone.0134551 (2015).
15. Janssen, A. W. F. et al. Transport of perfluoroalkyl substances across human induced pluripotent stem cell-derived intestinal epithelial cells in comparison with primary human intestinal epithelial cells and Caco-2 cells. *Arch. Toxicol.* https://doi.org/10.1007/s00204-024-03851-x (2024).
16. Poetsch, M. S., Strano, A. & Guan, K. Human induced pluripotent stem cells: From cell origin, genomic stability, and epigenetic memory to translational medicine. *Stem Cells* **40**, 546–555. https://doi.org/10.1093/stmcls/sxac020 (2022).

17. Kabeya, T. et al. Pharmacokinetic functions of human induced pluripotent stem cell-derived small intestinal epithelial cells. *Drug Metab. Pharmacokinet.* **35**, 374–382. https://doi.org/10.1016/j.dmpk.2020.04.334 (2020).
18. Kabeya, T. et al. Cyclic AMP signaling promotes the differentiation of human induced pluripotent stem cells into intestinal epithelial cells. *Drug Metab. Dispos.* **46**, 1411–1419. https://doi.org/10.1124/dmd.118.082123 (2018).
19. Zhao, W., Peng, C., Sakandar, H. A., Kwok, L. Y. & Zhang, W. Meta-analysis: Randomized trials of *Lactobacillusplantarum* on immune regulation over the last decades. *Front. Immunol.* **12**, 643420. https://doi.org/10.3389/fimmu.2021.643420 (2021).
20. van Baarlen, P. et al. Differential NF-kappaB pathways induction by *Lactobacillusplantarum* in the duodenum of healthy humans correlating with immune tolerance. *Proc. Natl. Acad. Sci. USA* **106**, 2371–2376. https://doi.org/10.1073/pnas.0809919106 (2009).
21. Wang, X., Spandidos, A., Wang, H. & Seed, B. PrimerBank: a PCR primer database for quantitative gene expression analysis, 2012 update. *Nucleic Acids Res.* **40**, D1144-1149. https://doi.org/10.1093/nar/gkr1013 (2012).
22. Angel, P. W. et al. A simple, scalable approach to building a cross-platform transcriptome atlas. *PLoS Comput. Biol.* **16**, e1008219. https://doi.org/10.1371/journal.pcbi.1008219 (2020).
23. Elzinga, J. et al. Systematic comparison of transcriptomes of Caco-2 cells cultured under different cellular and physiological conditions. *Arch. Toxicol.* **97**, 737–753. https://doi.org/10.1007/s00204-022-03430-y (2023).
24. Karki, R. & Kanneganti, T. D. The "cytokine storm": Molecular mechanisms and therapeutic prospects. *Trends Immunol.* **42**, 681–705. https://doi.org/10.1016/j.it.2021.06.001 (2021).
25. Pedersen, G. Development, validation and implementation of an in vitro model for the study of metabolic and immune function in normal and inflamed human colonic epithelium. *Dan Med. J.* **62**, B4973 (2015).
26. Wang, F. et al. Interferon-gamma and tumor necrosis factor-alpha synergize to induce intestinal epithelial barrier dysfunction by up-regulating myosin light chain kinase expression. *Am. J. Pathol.* **166**, 409–419. https://doi.org/10.1016/s0002-9440(10)62264-x (2005).
27. Wang, F. et al. IFN-gamma-induced TNFR2 expression is required for TNF-dependent intestinal epithelial barrier dysfunction. *Gastroenterology* **131**, 1153–1163. https://doi.org/10.1053/j.gastro.2006.08.022 (2006).
28. Meyer, F., Wendling, D., Demougeot, C., Prati, C. & Verhoeven, F. Cytokines and intestinal epithelial permeability: A systematic review. *Autoimmun Rev.* **22**, 103331. https://doi.org/10.1016/j.autrev.2023.103331 (2023).
29. Eiteman, M. A. & Ramalingam, S. Microbial production of lactic acid. *Biotechnol. Lett.* **37**, 955–972. https://doi.org/10.1007/s10529-015-1769-5 (2015).
30. Herath, M., Hosie, S., Bornstein, J. C., Franks, A. E. & Hill-Yardin, E. L. The role of the gastrointestinal mucus system in intestinal homeostasis: Implications for neurological disorders. *Front. Cell Infect. Microbiol.* **10**, 248. https://doi.org/10.3389/fcimb.2020.00248 (2020).
31. Van Tassell, M. L. & Miller, M. J. Lactobacillus adhesion to mucus. *Nutrients* **3**, 613–636. https://doi.org/10.3390/nu3050613 (2011).
32. Karczewski, J. et al. Regulation of human epithelial tight junction proteins by *Lactobacillusplantarum* in vivo and protective effects on the epithelial barrier. *Am. J. Physiol. Gastrointest. Liver Physiol.* **298**, G851-859. https://doi.org/10.1152/ajpgi.00327.2009 (2010).
33. Chuah, L. O. et al. Postbiotic metabolites produced by *Lactobacillusplantarum* strains exert selective cytotoxicity effects on cancer cells. *BMC Complement Altern. Med.* **19**, 114. https://doi.org/10.1186/s12906-019-2528-2 (2019).
34. Seddik, H. A. et al. *Lactobacillusplantarum* and its probiotic and food potentialities. *Probiotics Antimicrob. Proteins* **9**, 111–122. https://doi.org/10.1007/s12602-017-9264-z (2017).
35. Mazziotta, C., Tognon, M., Martini, F., Torreggiani, E. & Rotondo, J. C. Probiotics mechanism of action on immune cells and beneficial effects on human health. *Cells* **12**, 184. https://doi.org/10.3390/cells12010184 (2023).
36. Wells, J. M. Immunomodulatory mechanisms of lactobacilli. *Microb Cell Fact* **10 Suppl 1**, S17. https://doi.org/10.1186/1475-2859-10-s1-s17 (2011).
37. Daghero, H. et al. Jejunum-derived NF-κB reporter organoids as 3D models for the study of TNF-alpha-induced inflammation. *Sci. Rep.* **12**, 14425. https://doi.org/10.1038/s41598-022-18556-3 (2022).
38. Kurata, A. et al. Characterization of extracellular vesicles from *Lactiplantibacillusplantarum*. *Sci. Rep.* **12**, 13330. https://doi.org/10.1038/s41598-022-17629-7 (2022).
39. Hentschel, V., Seufferlein, T. & Armacki, M. Intestinal organoids in coculture: Redefining the boundaries of gut mucosa ex vivo modeling. *Am. J. Physiol. Gastrointest. Liver Physiol.* **321**, G693-g704. https://doi.org/10.1152/ajpgi.00043.2021 (2021).

Acknowledgements

We thank Jacco Spoelder for technical assistance with *Lactiplantibacillus plantarum* WCFS1 experiments.

Author contributions

A.J., A.P.V., S.B., P.B., L.F., M.Z. conceived and designed research; L.D., M.T., J.V., E.B., G.H. performed experiments, A.J., B.L., L.D., A.P.V., S.B., M.T., M.Z. analyzed data and interpreted results of experiments, B.L. drafted manuscript, A.J., M.Z., L.D., G.H., A.P.V., S.B., P.B. and L.F. edited and revised manuscript; all authors approved the final version of the manuscript.

Funding

This research was supported by the Dutch ministries of Agriculture, Nature and Food Quality (Grant: KB37-001-003) and Economic affairs via a Public Private Partnership grant from the Top consortium for Knowledge and Innovation (TKI) Agri & Food (Grant: LWV19125). The funding agencies had no role in the collection, analyses, and interpretation of data; nor in the preparation, review, or approval of the manuscript. The following companies contributed to the funding of this project: Mimetas, Micronit, Nestlé, STEMCELL Technologies and Stichting Proefdiervrij. These private partners, except Nestlé, had also no role in collection, analysis, and interpretation of data, or preparation of the manuscript.

Declarations

Competing interests

The authors declare no competing interests.

Additional information

Supplementary Information The online version contains supplementary material available at https://doi.org/10.1038/s41598-024-74802-w.

Correspondence and requests for materials should be addressed to M.v.d.Z.